Polymer 194 (2020) 122386

Contents lists available at ScienceDirect

Polymer

journal homepage: http://www.elsevier.com/locate/polymer

Chemical modification of atactic polypropylene and its applications as a crystallinity additive and compatibility agent

Meng-Heng Wu [a], Cheng-Chien Wang [b], Chuh-Yung Chen [a,*]

[a] Department of Chemical Engineering, National Cheng Kung University, 70101, Tainan, Taiwan, ROC
[b] Department of Chemical and Materials Engineering, Southern Taiwan University of Science and Technology, 71005, Tainan, Taiwan, ROC

ARTICLE INFO

Keywords:
Atactic polypropylene
Grafting polymerization
Blending

ABSTRACT

Maleic anhydride grafted onto atactic polypropylene (aPP-g-MAH) using a solution grafting reaction with ε-caprolactam promoter was investigated in this study. FTIR-ATR and elemental analysis (EA) measurements showed that the optimal degree of grafting (DG) of aPP-g-MAH could be achieved at a 5.03 wt% when ε-caprolactam was added as the radical protecting agent. aPP-g-MAH was then introduced to PP and PP/Nylon 6 (PP/Ny6) as a nucleation and compatibility agent, respectively. The DSC curve of the PP/aPP-g-MAH blend showed that the crystallization temperature of the blend was increased to 115.3 °C, higher than that of pristine PP. In addition, POM observations demonstrated that the size of the spherulites present in pristine PP shrank obviously. Moreover, the dynamic temperature variations in the POM observations revealed that the initial crystallization temperature of PP/aPP-g-MAH was much higher than that of pristine PP. The results indicate that the aPP-g-MAH additive was an excellent nucleating agent for the PP materials. When aPP-g-MAH was added as a compatibility agent for PP/Ny6 blending, the cryogenically fractured surface of the PP/Ny6/aPP-g-MAH (5 wt%) blend presented good compatibility between PP and the Ny6 domains. The crystallization temperatures of PP/Ny6 blends with 10–50 wt% Ny6 were higher than that of pure PP, and the blends with aPP-g-MAH had much higher of that. These findings reveal that aPP-g-MAH is a good nucleation and compatibility agent in PP/Ny6 blends.

1. Introduction

Polypropylene (PP) is one of the most important polymers in commodity plastics not only for its widely used in industry and commodity materials, but also for it was a low carbon-feet material. Nevertheless, the non-polarity of PP results in very poor compatibility and adhesion with other materials and thus restricts its application [1–6]. Many researchers have attempted to graft maleic anhydride (MAH) onto PP to improve the interfacial adhesion between PP and different components, such as polymers, metals and inorganic fillers in polymer blends [2]. In addition, the different types of PP, such as isotactic polypropylene (iPP) and atactic polypropylene (aPP), have been modified by MAH and used as compatible agents for strengthening the mechanical properties of composites based on PP [7–13].

Unfortunately, it is difficult to propagate the MAH monomer repeating unit during free radical grafting polymerization [1–4]. The degree of grafting (DG) of MAH onto a polymer depends on amount of active sites and its active life. Garcia-Martinez et al. [2] concluded that there is a maximum DG for MAH grafted onto PP regardless of how the initial concentration of MAH and/or peroxides in the grafting reaction system are regulated. To overcome the grafting limitation problem, some researchers have proposed different methods, including controlling the tacticity of the PP backbone [2,3], adding a second component to the reaction mixture [2,4,13–18], or reacting in different types of solvents [19,20]. For example, Garcia-Martinez et al. [3] reported that the absence of stereoregularity in PP could increase the DG by up to 4.2%. Garcia-Martinez et al. [21,22] also modified aPP in both batch solution and molten state process. The maximum DG of MAH onto aPP was 3.0% produced by Anirban Bhattacharya et al. [23] under a batch molten state process. Grafting modifications carried out photochemically were employed by Jun Qian et al. [24], and the DG was raised to approximately 4.0%. Antioxidant, as a radical scavenger, was added to the reaction medium to avoid collateral reactions, specifically β-scission, by Frantisek Kucera et al. [25] Diop et al. also modified PP with MAH using solid-state shear pulverization, achieving a significant amount of grafting and strongly suppressing β-scission, inhibiting molecular

* Corresponding author.
E-mail address: ccy7@mail.ncku.edu.tw (C.-Y. Chen).

https://doi.org/10.1016/j.polymer.2020.122386
Received 16 November 2019; Received in revised form 12 March 2020; Accepted 16 March 2020
Available online 17 March 2020
0032-3861/

weight reduction [26]. Incorporating p-(3-butenyl)toluene comonomer units into PP and then grafted 1.1% of MAH was presented by Min Zhang et al. [5] Li et al. [4] proposed that adding extra monomer, such as styrene (St), could assist in reducing the chain scission reaction and increased the DG of MAH onto PP from 0.25% to approximately 2.0%. Weihua Luo et al. [14] also claimed that grafting MAH in the presence of α-methyl-styrene could efficiently improve the amount of grafting on PP and prevent the excessive degradation of PP macromolecules. In addition, the effect of solvent on radical grafting polymerization has also been demonstrated [3,19,27]. Overall, the strategy of the above studies was to prolong the radical life and activity to improve the DG of MAH on aPP.

In recent decades, the mechanical properties of PP/Nylon 6 blends have been paid more attentions. PP is a versatile polymer due to its low material cost, high service temperature, high tensile modulus and good chemical resistance, but the low impact strength limits its applications. Nylon 6 has the advantages of easy processing, low friction, and suitable wear resistance, but it still has some disadvantages like high material cost, brittleness, poor dimensional stability, and considerable moisture absorption. The PP/Nylon6 blends could combine the merits and eliminate the shortcomings of them. However, it is worth noting that the incompatibility between PP and Nylon 6 form obvious phase separation leading to poor mechanical properties. Therefore, maleic anhydride grafted polypropylene (PP-*g*-MAH) was used as a compatibilizer to improve the miscibility of PP and Nylon 6 [7,12,28–30]. J. Roeder et al. [28] claimed that the addition of small quantities of PP-g-MAH to PP/Nylon 6 improve the compatibility with a reduction in the size of Nylon 6 domains and copolymer formation at the interface. Garcia-Martinez et al. [31] also proposed that aPP-g-MAH was an effective interfacial agent in PP/Nylon 6 blend. In addition, thermal behavior of PP/Nylon 6/aPP-g-MAH composites also studied by E. P. Collar et al. [32], and there is a critical value in the coupling agent level that optimizes the properties of the blend was found.

In our previous study, a novel radical system was constructed using mercaptan/ε-caprolactam (Cap) [33–37]. In this novel system, Cap plays an important role stabilizing the radicals and acting as a fragment at the polymer chain end. Hence, Cap was added to the MAH-aPP grafting system to prolong the radical life and improve the DG of aPP in this study. Furthermore, different solvents were chosen to change the environment of the reaction for the free radical grafting of MAH onto aPP with Cap additives. Finally, MAH grafted onto aPP (aPP-g-MAH) was applied to act as the nucleating agent for PP crystallinity improvement and the coupling agent for PP/Nylon blending.

2. Experimental

2.1. Materials

Maleic anhydride (MAH, 98%, Alfa Aesar Co. Ltd.), benzoyl peroxide (BPO, 97%, Alfa Aesar Co. Ltd.), and ε-caprolactam (99%, Alfa Aesar Co. Ltd.) were purified using recrystallization (twice) in solvent and were stored in a refrigerator before use. aPP ($\rho = 0.85$ g/cm^3, $M_w = 29{,}600$) and PP (YUNGSOX 1080; $\rho = 0.90$ g/cm^3, $M_w = 169{,}500$; melt flow index (MFI) = 10 g/10 min) were supplied by Formosa Plastics Corporation, Kaohsiung, Taiwan. Nylon 6 (Akulon F223D; $\rho = 1.13$ g/cm^3, $M_w = 19{,}546$; MFI = 44 g/10 min) was provided by DSM Engineering Plastics. Xylene (≥98.5%, Sigma-Aldrich Co. Ltd.), chlorobenzene (≥99.5%, J.T. Baker Co. Ltd.), and benzene (99%, Alfa Aesar Co. Ltd.) were used as received.

2.2. Grafting reaction of aPP with MAH

The grafting reaction was carried out in a three-necked Pyrex bottle equipped with a stirrer and a refluxing column. When using benzene as a solvent, the reaction was conducted in a high pressure reactor, the pressure of which was maintained at about 10 kgf/cm^2 by nitrogen gas. In section 3.1.1 and 3.1.4, xylene was selected as solvent for grafting reaction. Xylene, chlorobenzene, and benzene were used in section 3.1.2. All of reaction components, including aPP (16% w/v), MAH (7.8% w/v), with or without Cap addition, were dissolved in solvent and purged with nitrogen gas for 30 min and controlled at 120 °C. The BPO initiator solution was slowly titrated into the reactor. After 4 h, the reaction was terminated by precipitating in methanol, and the product was washed and purified several times in methanol. The final product, termed aPP-g-MAH, was dried under vacuum and stored in a dried box before used.

2.3. Blending process

The blends of PP containing 1 wt% aPP and 1, 5, or 10 wt% aPP-g-MAH were melted and blended in a Leistritz co-rotating twin screw extruder (diameter D = 27 mm and L/D = 36). PP was dried in an oven at 110 °C for 16 h to remove residual water before use. The temperature profile in extruder blocks was 120, 140, 160, 180, 180, 180, 180, 180,170, and 160, respectively. The gear rate and the compounding time in the intruder was 150 rpm and about 2 min, respectively. The PP/Nylon 6 composites were also manufactured by a Leistritz co-rotating twin screw extruder, and the temperature profile of the PP/Nylon 6 composites was 140, 160, 180, 200, 220, 220, 220, 220,210, and 200 °C, respectively. The gear rate was also controlled at 150 rpm.

2.4. Characterization

The samples were dissolved and precipitating several times as a wax like sample. Then, the samples were dried in vacuum under 80 °C to prevent the influence of water vapor. Next, the aPP and aPP-g-MAH were grinded with pestle and portar and analysed by attenuated total reflection (ATR) sampling accessory. The samples were analysed by FTIR-ATR (JASCO ATR-61) over the range of 700–4000 cm^{-1} with a spectrum resolution of 4 cm^{-1}. The spectra were averaged over 64 scans at room temperature. To precisely confirm the amount of grafted MAH and the DG of MA on aPP, elemental analysis (EA, Elementar Vario EL III) was carried out to identify the composition of C, H and O elements in the samples. The polarity changes of aPP and modified aPP were determined by contact angle (CA) measurement. The samples were made into a film by a hot-pressing process (190 °C for 10 min). The thermal properties of the samples (approximately 5 mg) were measured using differential scanning calorimetry (DSC, TA Instruments Q2000) under nitrogen purging. The heating and cooling rate of the test was controlled at 10 °C/min. The crystallization temperature of the samples was taken from the 2nd heating/cooling curves of DSC. A polarized optical microscope (POM, Olympus BH-2) equipped with a Linkam Scientific Instruments CI 93 temperature controller and a THMS 600 heating stage was employed to observe the crystallization behavior of the samples. The samples observed by POM were heated to melt, held for 10 min at 200 °C, at first. After the thermal history of the materials were eliminated, the cooling rate of samples was controlled at 10 °C/min to 60 °C. A JSM 6700F field emission scanning electron microscope (FESEM, JEOL, Japan) was used to observe the morphology of the cryogenically fractured surface and phase domains in the samples. (The composites extruded by extruder were quenched with liquid nitrogen for 5 min. After the treatment in liquid nitrogen, the composites became hard and brittle. The low temperature composites were broken by external force, and the fractured surfaces were observed under SEM.) For SEM analysis, the samples were prepared with a thin Pt film deposited on the samples via vacuum plating to enhance the sample conductivity and increase the SEM resolution. The Pt deposition was operated for 150 s under a pressure of 3.5 Pa at 10 mA.

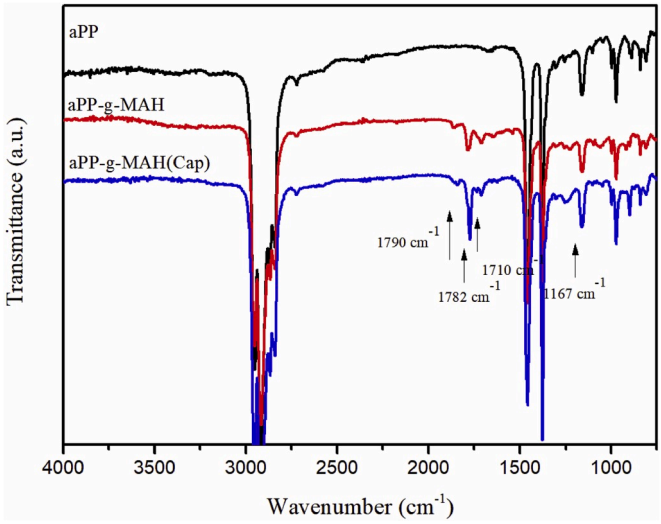

Fig. 1. FTIR-ATR spectra of (a) aPP, (b) aPP-g-MAH, and (c) aPP-g-MAH (Cap).

Table 1
Carbonyl index (CI = $\mathbf{A_{1782}/A_{1167}}$) of aPP, aPP-g-MAH, and aPP-g-MAH (Cap).

Sample	A_{1782}/A_{1167}
aPP	0
aPP-g-MAH	0.61
aPP-g-MAH (Cap)	0.97

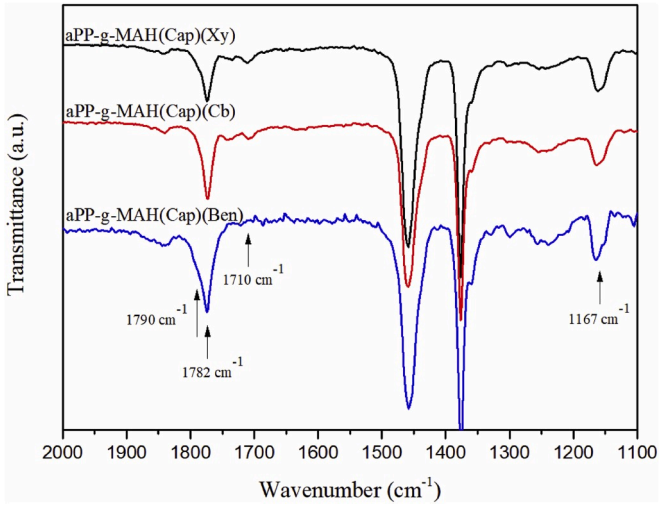

Fig. 2. FTIR-ATR spectra of aPP-g-MA using (a) xylene, (b) chlorobenzene, and (c) benzene as the reaction medium.

Table 2
CI of aPP-g-MA prepared using xylene, chlorobenzene, and benzene as reaction media.

Sample	A_{1782}/A_{1167}
aPP-g-MAH (Cap)(Xy)	0.97
aPP-g-MAH (Cap)(Cb)	1.21
aPP-g-MAH (Cap)(Ben)	1.56

Table 3
DG and contact angle (CA) of aPP, aPP-g-MAH, aPP-g-MAH (Cap)(Xy), aPP-g-MA (Cap)(Cb), and aPP-g-MAH (Ben).

Sample	C[a] (wt%)	H[a]	O[b]	DG	CA
aPP	85.56	14.44	0	0.00	110°
aPP-g-MAH	84.61	14.11	1.28	2.62	109°
aPP-g-MAH (Cap)(Xy)	84.34	13.97	1.69	3.59	103°
aPP-g-MAH (Cap)(Cb)	84.11	13.94	1.95	3.93	98°
aPP-g-MAH (Cap)(Ben)	83.82	13.86	2.32	4.90	97°

[a] The contents of C and H were determined by using an elementary analyzer.
[b] Calculated from the C and H contents.

3. Results and discussion

3.1. Maleic anhydride grafted onto atactic polypropylene

3.1.1. Grafting of MAH onto aPP with and without Cap

The FTIR-ATR spectra of pristine aPP, aPP-g-MAH and aPP-g-MAH (Cap) are shown in Fig. 1. The absorption bands at 1782 and 1790 cm^{-1} assigned to carbonyl groups (-C═O) of MAH were present in both aPP-g-MAH and aPP-g-MAH (Cap). The shoulder bands shown at 1710 cm^{-1} were assigned to carbonyl groups of carboxylic acids. The lack of a broad band in the range of 3200 cm^{-1} - 3600 cm^{-1} illustrated that the anhydride group of MAH grafted onto aPP did not open the ring to form a carboxylic acid group [1,4]. According to previous studies [1], the carbonyl index (CI = $\mathbf{A_{1782}/A_{1167}}$), which is the area ratio of the characteristic peaks of anhydride at 1782 cm^{-1} to methyl groups at 1167 cm^{-1}, can be used to estimate the DG of MAH onto aPP. Table 1 shows that the CI of MAH grafted onto aPP was 0.97 and 0.61, respectively, with and without Cap addition. This result clearly indicates that the DG of MAH onto aPP was significantly improved by the addition of Cap due to the radical protection function of Cap. Cap acts as a dormant species that can dissociate reversibly into active radicals to maintain radical activity, according to our previous study [20]. The role of Cap in the reaction was also shown in Scheme S1 in supplementary data. Fig. 1 also reveals that the aPP-g-MAH had two peaks, at 1790 cm^{-1} and 1782 cm^{-1}, both of which are attributed to the grafted single succinic anhydride unit attached to the chain end of aPP and poly(maleic anhydride) or to other forms of MAH, according to literature reports [4,38]. In particular, the characteristic peak at 1790 cm^{-1} in aPP-g-MAH(Cap) had nearly disappeared, which indicated that fewer single MAH molecules were grafted onto the chain end of aPP when Cap was added to the grafting system. This result reveals that dormant Cap species can inhibit MAH grafting onto the chain end of aPP.

3.1.2. Solvent effect

Different solvents, including xylene (Xy), chlorobenzene (Cb) and benzene (Ben), were used as the reaction medium to evaluate the DG of MAH grafting onto aPP. The FTIR-ATR spectra and CI values of aPP-g-MAH(Cap)(Xy), aPP-g-MAH(Cap)(Cb) and aPP-g-MAH(Cap)(Ben) are shown in Fig. 2 and Table 2, respectively. The absorption band at 1782 cm^{-1} for the MAH group was present in all sample spectra, indicating that all aPP samples had successfully grafted MAH onto the main chain. The CI of aPP-g-MAH(Cap)(Cb) was obviously higher than that of aPP-g-MAH(Cap)(Xy). This result indicates that the probability of radicals transferring to the solvent, as well as chain transfer, is inhibited in a system with chlorobenzene as solvent, because two methyl groups of xylene are highly reactive with radicals in the polymerization [20]. Xylene would transfer the free radicals of primary radicals from initiator and macroradicals from to itself. These reactions may greatly suppress the grafting reaction and reduce the degree of grafting. The amount of MAH grafted onto aPP-g-MAH(Cap)(Ben) was the highest owing to the stable chemical structure of benzene [19]. Benzene, with symmetrical and stable chemical structure, was much more stable relative to xylene

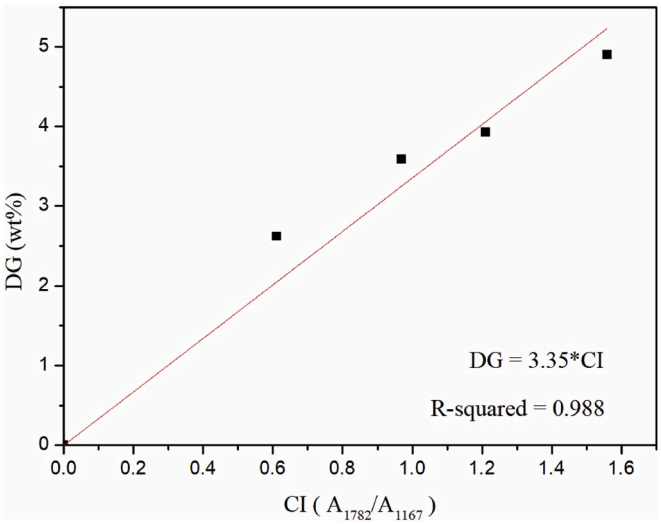

Fig. 3. The relationship between CI and DG in the aPP-g-MAH samples.

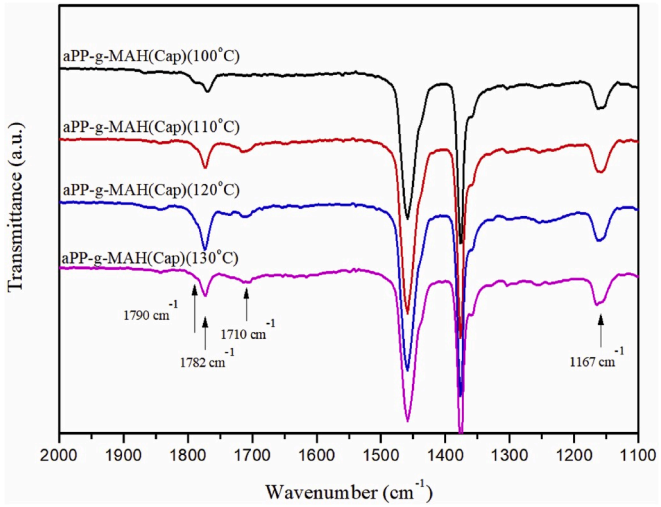

Fig. 4. FTIR-ATR spectra of aPP-g-MAH (Cap) prepared at (a) 100 °C, (b) 110 °C, (c) 120 °C and (d) 130 °C.

Table 4
Carbonyl index of aPP-g-MAH(Cap) prepared at 100 °C, 110 °C, 120 °C and 130 °C.

Sample	A_{1782}/A_{1167}	DG[a]
aPP-g-MAH (Cap)(100 °C)	0.56	1.88
aPP-g-MAH (Cap)(110 °C)	0.68	2.28
aPP-g-MAH (Cap)(120 °C)	0.97	3.25
aPP-g-MAH (Cap)(130 °C)	0.81	2.71

[a] Calculated by CI.

and chlorobenzene. In addition, the chain transfer reaction would be greatly inhibited on it. Therefore, benzene is the best choice of reaction solvent to increase the DG of aPP-g-MAH [19,20].

3.1.3. The DG of aPP-g-MAH

The DG of aPP-g-MAH samples was further detected and calculated from the results of elementary analysis (EA), as shown in Table 3. The trend of DG obtained from EA data for the aPP-g-MAH samples was consistent with the CI value, as shown in Table 3 and Fig. 3. The notable linear relationship of CI and DG, with an R-squared value of 0.988, is

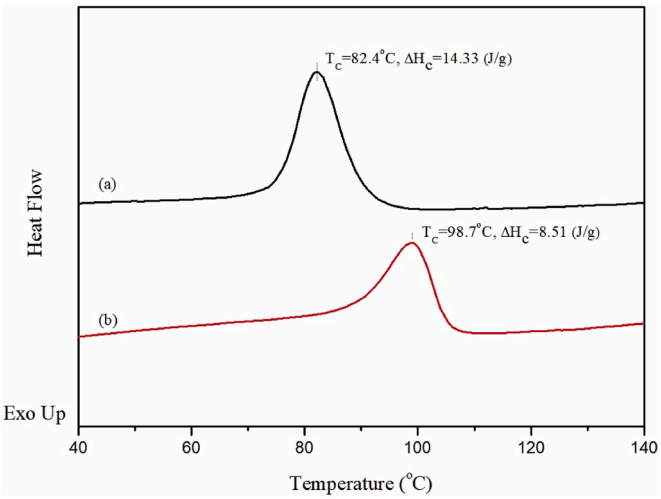

Fig. 5. DSC cooling curves for (a) aPP and (b) aPP-g-MAH(Cap)(Ben).

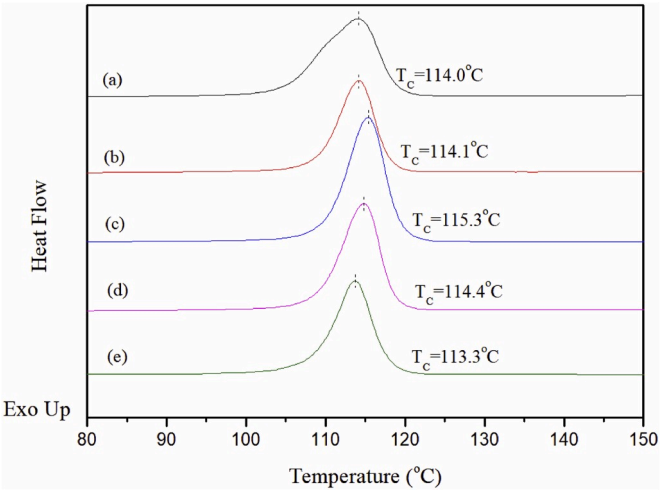

Fig. 6. DSC cooling curves for (a) PP, (b) PP/aPP = 99/1, (c) PP/aPP-g-MAH (Cap)(Ben) = 99/1, (d) PP/aPP-g-MAH(Cap)(Ben) = 95/5, and (e) PP/aPP-g-MAH(Cap)(Ben) = 90/10.

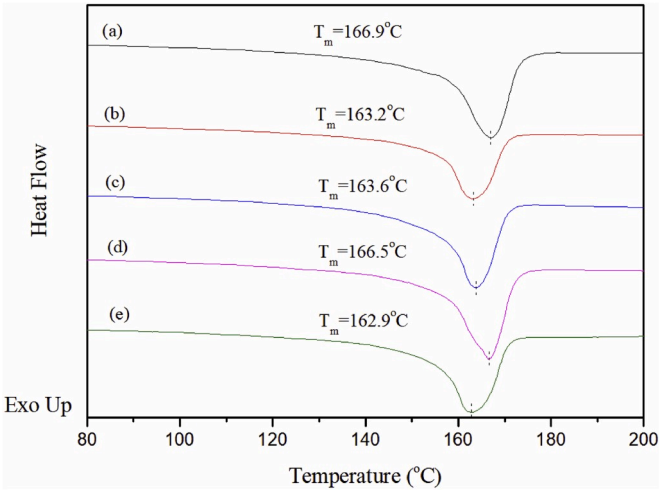

Fig. 7. DSC heating curves for (a) PP, (b) PP/aPP = 99/1, (c) PP/aPP-g-MAH (Cap)(Ben) = 99/1, (d) PP/aPP-g-MAH(Cap)(Ben) = 95/5, and (e) PP/aPP-g-MAH(Cap)(Ben) = 90/10.

Table 5
Thermal properties of the PP/aPP and the PP/aPP-g-MAH blends.

Sample	T_c (°C)	ΔH_c (J/g)	T_m (°C)	ΔH_m (J/g)
PP	114.0	86.5	166.9	83.5
PP/aPP = 99/1	114.1	86.8	163.2	85.6
PP/aPP-g-MAH (Cap)(Ben) = 99/1	115.3	97.1	163.6	92.4
PP/aPP-g-MAH (Cap)(Ben) = 95/5	114.4	92.4	166.5	88.3
PP/aPP-g-MAH (Cap)(Ben) = 90/10	113.3	88.3	162.9	83.6

displayed in Fig. 3. From the slope of linear curve in Fig. 3, the DG of aPP-g-MAH samples can be obtained by 3.5 times the CI value. This result illustrates that the CI value can represent the DG of aPP-g-MAH. In addition, the contact angle (CA) displayed in Table 3 shows a higher DG of aPP-g-MAH with a lower CA, because the hydrophobicity of aPP decreased with an increasing DG of aPP-g-MAH [39]. Without any modification, the CA of aPP is approximately 110°. The CA of aPP-g-MAH was decreased to 97°, as its DG was 4.9 wt%. This polarity change indicates that aPP-g-MAH is a good coupling agent for PP blending with a polar polymer, such as Nylon.

3.1.4. Temperature effect

The effect of the reaction temperature on the DG of MAH onto aPP was explored, as shown in Fig. 4 and Table 4. The CI values of aPP-g-MAH prepared at 100 °C, 110 °C, 120 °C and 130 °C were 0.56, 0.68, 0.97 and 0.81, respectively. The optimum temperature of the grafting reaction was 120 °C, as deduced from the CI value. When the reaction temperature was increased to greater than 120 °C, the lower CI of the aPP-g-MAH indicated that the DG of MAH on aPP was decreased. The

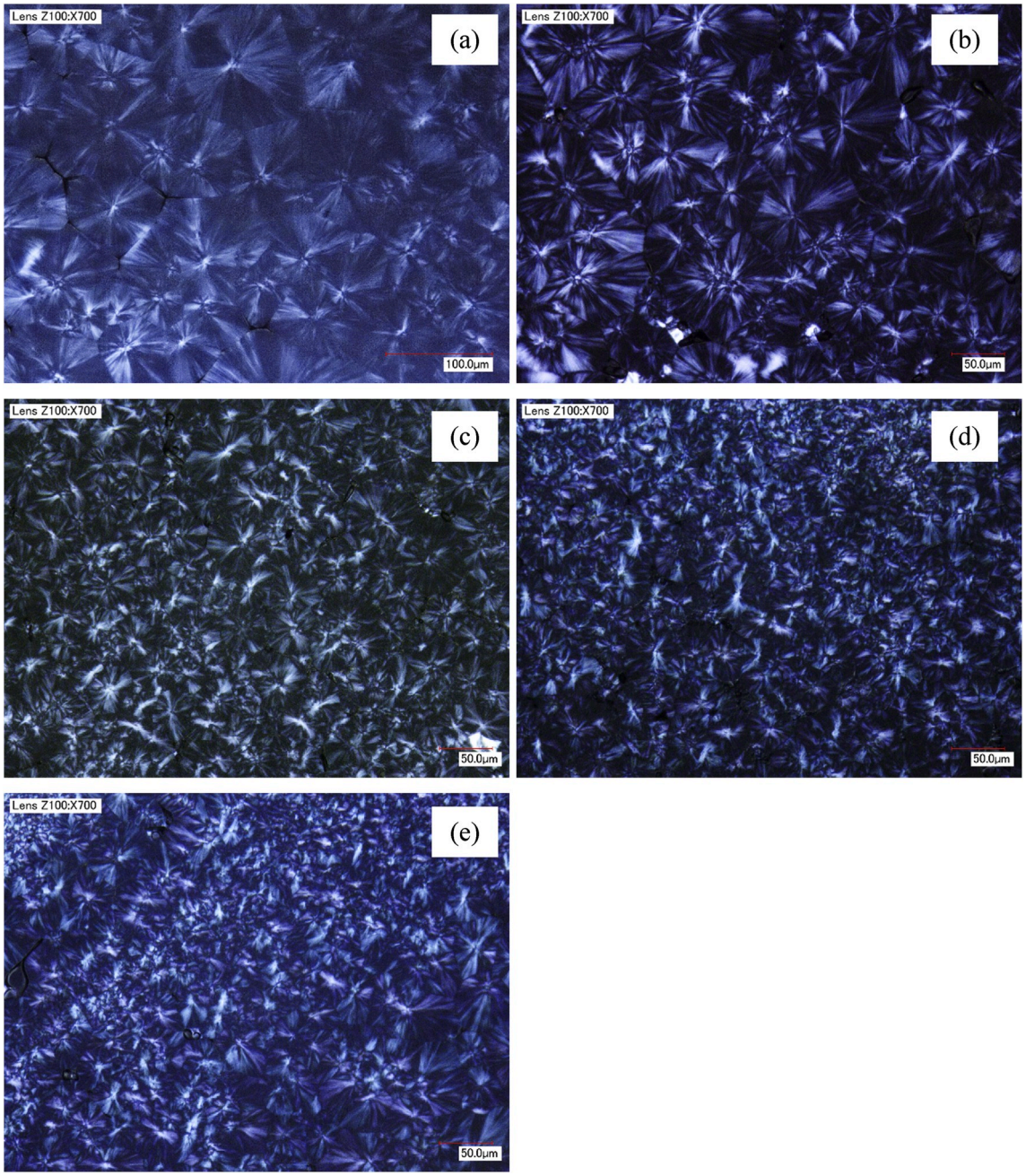

Fig. 8. POM images of (a) PP, (b) PP/aPP = 99/1, (c) PP/aPP-g-MAH(Cap)(Ben) = 99/1, (d) PP/aPP-g-MAH(Cap)(Ben) = 95/5, and (e) PP/aPP-g-MAH(Cap)(Ben) = 90/10.

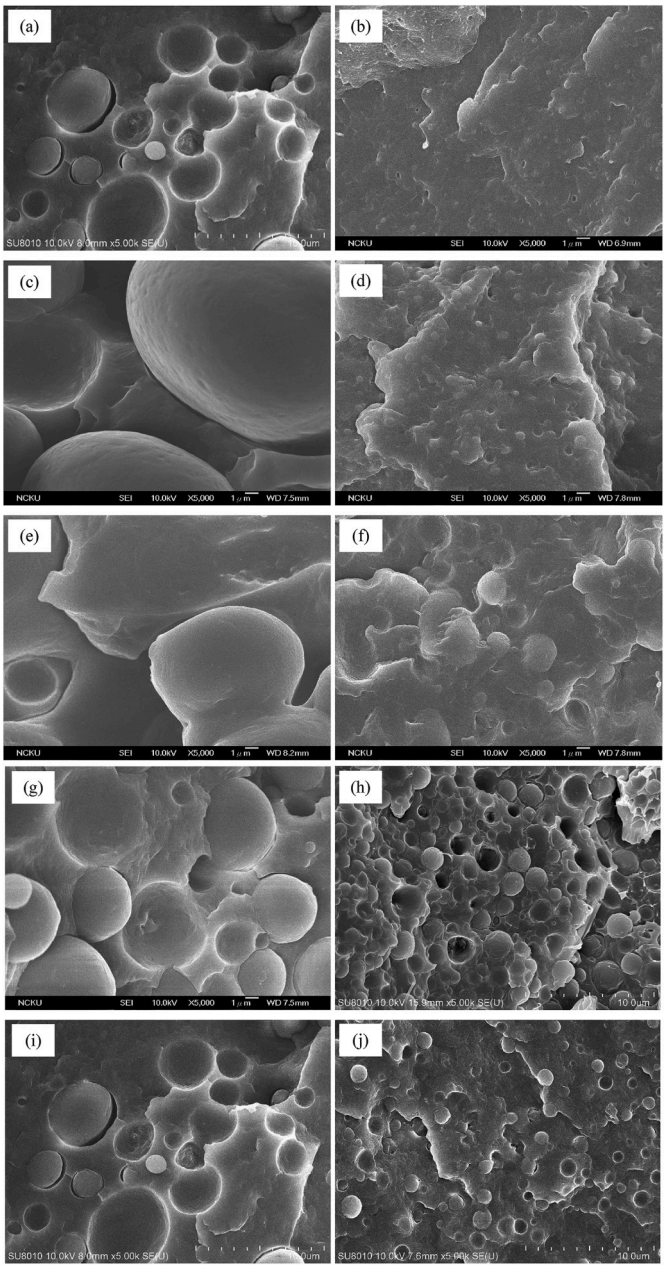

Fig. 9. SEM micrographs of (a) PP/Nylon6 = 90/10; (b) PP/Nylon6/aPP-g-MAH(Cap)(Ben) = 90/10/5; (c) PP/Nylon6 = 70/30; (d) PP/Nylon6/aPP-g-MAH(Cap)(Ben) = 70/30/5; (e) PP/Nylon6 = 50/50; (f) PP/Nylon6/aPP-g-MAH(Cap)(Ben) = 50/50/5; (g) PP/Nylon6 = 30/70; (h) PP/Nylon6/aPP-g-MAH(Cap)(Ben) = 30/70/5; (i) PP/Nylon6 = 10/90; and (j) PP/Nylon6/aPP-g-MAH(Cap)(Ben) = 10/90/5.

characteristic peak at 1790 cm^{-1}, which was attributed to a succinic anhydride attached to the chain end of aPP, also gradually disappeared as the grafting temperature was increased from 100 °C to 130 °C. These results indicated that the rate of termination reactions was greatly increased at temperatures above 120 °C [40], and the dormant species dissociation still occurred as the temperature increased above 100 °C.

3.2. Physical properties of aPP-g-MAH and PP/aPP-g-MAH blends

3.2.1. Crystallization behavior of aPP-g-MAH

The crystallization temperatures (T_c) of aPP and aPP-g-MAH(Cap)(Ben) were measured by DSC, as shown in Fig. 5. The low enthalpy of crystallization (ΔH_c) of aPP and aPP-g-MAH(Cap)(Ben) was due to the low tacticity. Moreover, the T_c of aPP-g-MAH (98.7 °C) was obviously higher than that of aPP (82.4 °C), indicating that aPP-g-MAH can crystallize more easily. Thus, aPP-g-MAH(Cap)(Ben) effectively acted as the nucleation site to induce the crystallization of aPP [41].

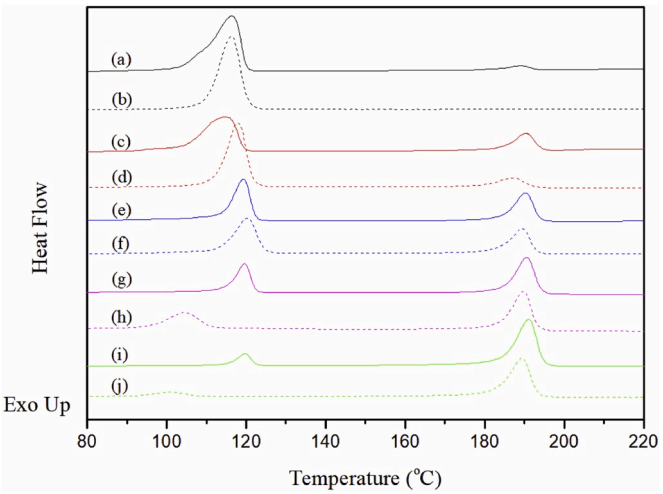

Fig. 10. DSC cooling curves for (a) PP/Ny6 = 90/10, (b) PP/Ny6/aPP-g-MAH(Cap)(Ben) = 90/10/5, (c) PP/Ny6 = 70/30, (d) PP/Ny6/aPP-g-MAH(Cap)(Ben) = 70/30/5, (e) PP/Ny6 = 50/50, (f) PP/Ny6/aPP-g-MAH(Cap)(Ben) = 50/50/5, (g) PP/Ny6 = 30/70, (h) PP/Ny6/aPP-g-MAH(Cap)(Ben) = 30/70/5, (i) PP/Ny6 = 10/90, and (j) PP/Ny6/aPP-g-MAH(Cap)(Ben) = 10/90/5.

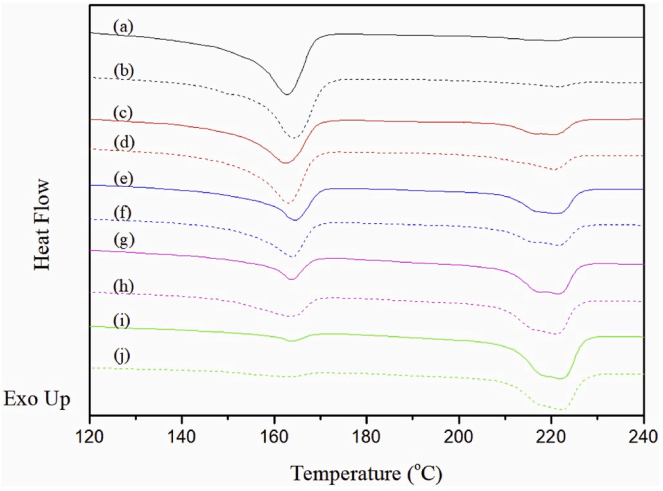

Fig. 11. DSC heating curves for (a) PP/Ny6 = 90/10, (b) PP/Ny6/aPP-g-MAH(Cap)(Ben) = 90/10/5, (c) PP/Ny6 = 70/30, (d) PP/Ny6/aPP-g-MAH(Cap)(Ben) = 70/30/5, (e) PP/Ny6 = 50/50, (f) PP/Ny6/aPP-g-MAH(Cap)(Ben) = 50/50/5, (g) PP/Ny6 = 30/70, (h) PP/Ny6/aPP-g-MAH(Cap)(Ben) = 30/70/5, (i) PP/Ny6 = 10/90, and (j) PP/Ny6/aPP-g-MAH(Cap)(Ben) = 10/90/5.

3.2.2. Thermal properties and crystallization behavior of PP/aPP-g-MAH blends

The DSC traces and thermal properties of the PP blends with 1 wt% aPP and 1 wt% aPP-g-MAH(Cap)(Ben) are shown in Fig. 6, Fig. 7 and Table 5, respectively. The T_c and ΔH_c values of the PP blended with 1 wt % aPP-g-MAH(Cap)(Ben) were higher than those of pristine PP and the PP/aPP blend. Notably, the crystallization peak of the PP/aPP-g-gMAH (Cap)(Ben) blend was narrower and stronger than that of pristine PP and the PP/aPP blend, suggesting a narrow size distribution of crystallites in the PP/aPP-g-gMAH(Cap)(Ben) blend (Fig. 6 (a) and (c)) [42]. These results revealed that the addition of aPP-g-MAH to PP enhanced the crystallization degree of PP due to the heterogeneous nucleation effect

Table 6
Thermal properties of PP/Ny6 and PP/Ny6/aPP-g-MAH composites.

Sample	T_c (°C)		T_m (°C)		ΔH_c (J/g)		ΔH_m (J/g)	
	PP	Ny6	PP	Ny6	PP	Ny6	PP	Ny6
PP/Ny6 = 90/10	116.3	189.1	162.8	220.3	78.9	4.7	79.5	4.4
PP/Ny6/aPP-g-MAH = 90/10/5	116.2	–	164.2	221.3	81.7	–	84.3	4.2
PP/Ny6 = 70/30	114.8	190.5	162.6	220.9	59.5	18.2	55.3	15.1
PP/Ny6/aPP-g-MAH = 70/30/5	118.0	187.1	163.1	220.7	68.1	13.7	64.2	14.8
PP/Ny6 = 50/50	119.2	190.2	164.4	221.1	42.4	30.4	36.1	26.5
PP/Ny6/aPP-g-MAH = 50/50/5	120.4	189.5	163.8	221.7	43.9	24.7	42.2	21.7
PP/Ny6 = 30/70	119.6	190.6	163.7	221.4	24.4	39.1	21.3	34.0
PP/Ny6/aPP-g-MAH = 30/70/5	104.6	189.8	163.7	221.0	25.7	40.7	21.7	36.0
PP/Ny6 = 10/90	119.6	191.0	163.8	222.2	9.2	52.9	7.3	47.7
PP/Ny6/aPP-g-MAH = 10/90/5	101.0	189.4	163.3	222.2	5.6	48.8	4.8	45.9

[41,42]. The T_c of the PP/aPP-g-gMAH(Cap)(Ben) blend with 1 wt% aPP-g-gMA(Cap)(Ben) increased from 114.0 °C to 115.3 °C. The ΔH_c and enthalpy of fusion (ΔH_m) of the PP/aPP-g-gMAH(Cap)(Ben) blend with 1 wt% aPP-g-gMAH(Cap)(Ben) were the highest values (97.1 and 92.4 J/g, respectively) among the different weighting PP/aPP-g-gMAH(Cap)(Ben) blends, indicating that it has the highest crystallinity. Due to the crystallinity, the PP and PP/aPP blend have similar peak strengths, as displayed in Fig. 7(a) and (b). The PP/aPP-g-gMAH(Cap)(Ben) blend with 1 wt% aPP-g-gMAH(Cap)(Ben) has the strongest peak (Fig. 7 (c)). However, when the amount of aPP-g-MAH(Cap)(Ben) within PP is greater than 5 wt%, the T_c and ΔH_c values began to decline due to interruptions from the excessive addition of aPP-g-MAH [43], as shown in Fig. 6. Chen et al. [43] also claimed that the nucleation and growth rates of the crystallization behavior for iPP are interrupted by the presence of aPP molecules. The interrupting phenomena could also be demonstrated in the broader peak and lower melting temperature of the exotherms shown in Fig. 7(d) and (e). The ΔH_c and ΔH_m values of the PP/aPP-g-gMAH(Cap)(Ben) blend with 5 wt% aPP-g-gMA(Cap)(Ben) were 92.4 and 88.3 (J/g), respectively. The ΔH_c and ΔH_m values of the PP/aPP-g-gMAH(Cap)(Ben) blend with 10 wt% aPP-g-gMA(Cap)(Ben) were 88.3 and 83.6 (J/g), respectively. The above values, which were much lower than the blend with 1 wt% aPP-g-MAH(Cap)(Ben), were also indicative of crystallization interruption.

The crystallization morphology of PP, PP/aPP and the PP/aPP-g-MAH blends were further observed by using POM with a heating stage, as shown in Fig. 8. The crystallization morphologies of pristine PP and the PP/aPP blend formed large spherulites with diameters of approximately 100 μm (Fig. 8(a)) as it cooled from the melting state. The spherulite size for the PP domain decreased with an increasing content of aPP-g-MAH(Cap)(Ben). Shrinking of the spherulite size may have arose from the large amount of heterogeneous nucleation sites induced by aPP-g-MAH(Cap)(Ben) [41,42]. In addition, the uniform distribution of the spherulites was in accordance with the narrow crystallization peak in the DSC curve. However, when the content of aPP-g-MAH within the PP domain was increased to 10 wt%, spherulites with a wide size distribution were observed (Fig. 8(e)). Although small-sized spherulites could be found, there were also large spherulites present. This phenomena could also be observed as the wider peak width of the PP/aPP-g-MAH(Cap)(Ben) = 90/10 crystallization peak in DSC. The wide size distribution of the spherulites may arise from some amount of phase segregation of aPP-g-MAH in the blend.

3.3. Miscible phenomena and thermal behavior of PP/Nylon 6/aPP-g-MAH blends

The compatibility between PP and Nylon 6 (Ny6) in the composites with and without aPP-g-MAH were first observed by SEM. The cryogenically fractured surfaces of PP with 10, 30, 50, 70 and 90 wt% Ny6 blend are shown in Fig. 9. Fig. 9 (a), (c), (e), (g) and (i) are the SEM micro-images of the PP/Nylon 6 blend, showing that the minor spherical phase was dispersed within the matrix owing to phase segregation. The voids with a sharp interface in the images were due to domains being extracted from the matrix during the fracture process, revealing that the interaction between PP and Ny6 is weak [7,12,29,30]. In contrast, as the 5 wt% aPP-g-MAH was added as a coupling agent between PP and Ny6, the blurred interface between PP and the Ny6 domains indicates that the compatibility of PP and Ny6 was efficiently promoted, as shown in Fig. 9 (b), (d), (f) and (j). In particular, for 10 wt% and 30 wt% of Ny6 blending with PP and aPP-g-MAH (Fig. 9 (b) and (d)), the spherical dispersion of Ny6 in PP was nearly absent, supporting the idea that aPP-g-MAH is suitable as a coupling agent for PP/Ny6 blending [7,12,29,30]. When the composition of Ny6 in the PP/Ny6 blends was increased to 50 wt%, 70 wt% and 90 wt% (Fig. 9(f), (h) and (j)), the amount of spherically dispersed phase became smaller and was well-dispersed in the matrix. Moreover, the morphology of the domains that were extracted during fracture indicated that aPP-g-MAH was not sufficient to act as a coupling agent in the presence of higher Ny6 contents [7,12,29,30].

The thermal properties of the PP/Ny6 and PP/Ny6/aPP-g-MAH(Cap)(Ben) blends were also characterized by DSC, as shown in Figs. 10 and 11. The temperature and latent heat of crystallization and melting are presented in Table 6. The DSC curves show that the crystallization peaks of PP and Ny6 without aPP-g-MAH are different in cooling and heating curves, indicating the phase segregation phenomenon. As aPP-g-MAH was added, the crystallization peak of Ny6 disappeared, showing good miscibility in the blend with 10 wt% Ny6 (Fig. 10 (b)) [7]. In addition, the crystallization peak of PP in PP/Ny6/aPP-g-MAH became stronger and narrower. The T_c of PP/Ny6/aPP-g-MAH(Cap)(Ben) = 90/10/5 ($T_{c,PP}$) was 116.2 °C (Table 6), which was 2.2 °C higher than the T_c of pristine PP (114.0 °C), revealing that the presence of Ny6 and aPP-g-MAH as a nucleating agent provoked the crystallization behavior of PP [7,42]. Similar phenomena could be found for PP/Ny6 = 70/30 and 50/50, with and without aPP-g-MAH, due to the presence of high-T_c Ny6 and aPP-g-MAH. The weaker promotion of ΔH_c in PP/Ny6/aPP-g-MAH(Cap)(Ben) = 50/50/5 relative to PP/Ny6 = 90/10 and 70/30 was due to the excessive additive of aPP-g-MAH, as mentioned for the PP/aPP-g-MAH blends. These results also showed that aPP-g-MAH has a relatively higher solubility in PP. In addition, the peaks of PP and Ny6 had separate melting endotherms, demonstrating that Ny6 and PP crystallize independently (Fig. 11(b)). The cooling curve of the PP/Ny6/aPP-g-MAH(Cap)(Ben) blend (70/30/5) showed a similar result (Figs. 10 and 11 (c) and (d)). When the proportion of PP/Ny6 was decreased to 30/70 and 10/90, the $T_{c,PP}$ values decreased to 104.6 and 101.0 °C, respectively, which were lower than the T_c values for pristine PP and PP/Ny6 without aPP-g-MAH, as shown in Table 6. The crystallization peaks of PP in the PP/Ny6/aPP-g-MAH(Cap)(Ben) = 30/70/5 and 10/90/5 also became broader, and the $T_{c,PP}$ of each shifted to a lower temperature, as presented in Table 6, Fig. 10(h) and (j). These poorer crystallization behaviors were due to the excessive addition of aPP-g-MAH, as previously mentioned. Apart from this, the totally separated crystallization peaks and melting peaks of PP and Ny6 (shown in Figs. 10 and 11(h) and (j)) demonstrated that the miscibility of these composites was not good relative to the composite with a lower content

of Ny6 [7]. In addition, the T_c, T_m, ΔH_c and ΔH_m of Ny6 in the PP/Ny6 blends showed no drastic changes with or without aPP-g-MAH, indicating that aPP-g-MAH had no effect on the crystallization of Ny6.

4. Conclusion

The DG of MAH onto aPP was greatly improved by the Cap radical protector and the use of benzene solvent. When 1 wt% aPP-g-MAH was added to PP, the crystallinity of PP was increased. However, when the content of aPP-g-MAH was raised to 5 wt% and 10 wt%, the T_c and ΔH_c values became lower owing to the interruptions of excess aPP-g-MAH. In addition, the compatibility between PP and Ny6 could be greatly enhanced by aPP-g-MAH additive. However, as the content of Ny6 was increased to 50% in the blends, the coupling agent of aPP-g-MAH lost its function in the PP/Ny6/aPP-g-MAH blend.

Declaration of competing interest

The authors declare that they have no known competing financial interests or personal relationships that could have appeared to influence the work reported in this paper.

CRediT authorship contribution statement

Meng-Heng Wu: Methodology, Software, Validation, Formal analysis, Investigation, Data curation, Writing - original draft, Writing - review & editing, Visualization. **Cheng-Chien Wang:** Methodology, Writing - review & editing. **Chuh-Yung Chen:** Conceptualization, Methodology, Resources, Writing - review & editing, Visualization, Supervision, Project administration, Funding acquisition.

Acknowledgements

The authors would like to thank the Ministry of Science and Technology of the Republic of China for financially supporting this work under Contract Nos. MOST 107-2823-8-006-007 and MOST 107-2221-E-006-002.

Appendix A. Supplementary data

Supplementary data to this article can be found online at https://doi.org/10.1016/j.polymer.2020.122386.

References

[1] S. Bettini, J. Agnelli, Evaluation of methods used for analysing maleic anhydride grafted onto polypropylene by reactive processing, Polym. Test. 19 (1) (2000) 3–15.
[2] J.M. García-Martínez, O. Laguna, E. Collar, Role of reaction time in batch process modification of atactic polypropylene by maleic anhydride in melt, J. Appl. Polym. Sci. 65 (7) (1997) 1333–1347.
[3] J.M. García-Martínez, O. Laguna, E. Collar, Chemical modification of polypropylenes by maleic anhydride: influence of stereospecificity and process conditions, J. Appl. Polym. Sci. 68 (3) (1998) 483–495.
[4] Y. Li, X.-M. Xie, B.-H. Guo, Study on styrene-assisted melt free-radical grafting of maleic anhydride onto polypropylene, Polymer 42 (8) (2001) 3419–3425.
[5] M. Zhang, R.H. Colby, S.T. Milner, T.M. Chung, T. Huang, W. Degroot, Synthesis and characterization of maleic anhydride grafted polypropylene with a well-defined molecular structure, Macromolecules 46 (11) (2013) 4313–4323.
[6] A. Oromiehie, H. Ebadi-Dehaghani, S. Mirbagheri, Chemical modification of polypropylene by maleic anhydride: melt grafting, characterization and mechanism, Int. J. Chem. Eng. Appl. 5 (2) (2014) 117.
[7] A. Tedesco, R. Barbosa, S. Nachtigall, R. Mauler, Comparative study of PP-MA and PP-GMA as compatibilizing agents on polypropylene/nylon 6 blends, Polym. Test. 21 (1) (2002) 11–15.
[8] S.J. Park, B.K. Kim, H.M. Jeong, Morphological, thermal and rheological properties of the blends polypropylene/nylon-6, polypropylene/nylon-6/(maleic anhydride-g-polypropylene) and (maleic anhydride-g-polypropylene)/nylon-6, Eur. Polym. J. 26 (2) (1990) 131–136.
[9] Q. Chen, Y. Deng, X. Mao, F. Yin, J. Lin, Preparation and reaction kinetics of polypropylene-graft-cardanol by reactive extrusion and its compatibilization on polypropylene/polystyrene, J. Appl. Polym. Sci. 131 (4) (2014).
[10] J.-S. Yeo, S.-H. Hwang, Preparation and characteristics of polypropylene-graft-maleic anhydride anchored micro-fibriled cellulose: its composites with polypropylene, J. Adhes. Sci. Technol. 29 (3) (2015) 185–194.
[11] J. Parameswaranpillai, G. Joseph, R.V. Chellappan, A.K. Zahakariah, N. Hameed, The effect of polypropylene-graft-maleic anhydride on the morphology and dynamic mechanical properties of polypropylene/polystyrene blends, J. Polym. Res. 22 (2) (2015) 2.
[12] N. Abacha, S. Fellahi, Synthesis of polypropylene-graft-maleic anhydride compatibilizer and evaluation of nylon 6/polypropylene blend properties, Polym. Int. 54 (6) (2005) 909–916.
[13] Z. Tian, L. Pan, Q. Pan, Polypropylene grafted with maleic anhydride and styrene as a compatibilizer for biodegradable poly (propylene carbonate)/polypropylene, J. Eng. Fibers Fabr. 14 (2019), 1558925019849714.
[14] W. Luo, X. Liu, Y. Fu, Melt grafting of maleic anhydride onto polypropylene with assistance of α-methylstyrene, Polym. Eng. Sci. 52 (4) (2012) 814–819.
[15] Q.L. Ni, J.Q. Fan, H. Niu, J.Y. Dong, Enhancement of graft yield and control of degradation during polypropylene maleation in the presence of polyfunctional monomer, J. Appl. Polym. Sci. 121 (5) (2011) 2512–2517.
[16] S. Augier, S. Coiai, T. Gragnoli, E. Passaglia, J.-L. Pradel, J.-J. Flat, Coagent assisted polypropylene radical functionalization: monomer grafting modulation and molecular weight conservation, Polymer 47 (15) (2006) 5243–5252.
[17] S. Coiai, S. Augier, C. Pinzino, E. Passaglia, Control of degradation of polypropylene during its radical functionalisation with furan and thiophene derivatives, Polym. Degrad. Stabil. 95 (3) (2010) 298–305.
[18] Y. Zhu, C. Liang, Y. Bo, S. Xu, Compatibilization of polypropylene/recycled polyethylene terephthalate blends with maleic anhydride grafted polypropylene in the presence of diallyl phthalate, J. Polym. Res. 22 (3) (2015) 35.
[19] C.J. Wu, C.Y. Chen, E. Woo, J.F. Kuo, A kinetic study on grafting of maleic anhydride onto a thermoplastic elastomer, J. Polym. Sci. Polym. Chem. 31 (13) (1993) 3405–3415.
[20] M. Ghaemy, S. Roohina, Grafting of maleic anhydride on polyethylene in a homogeneous medium in the presence of radical initiators, Iran. Polym. J. (Engl. Ed.) 12 (2003) 21–29.
[21] J.M. García-Martínez, S. Areso, E. Collar, The transient nature of maximum maleic anhydride grafting of polypropylene: a mechanistic approach based on a consecutive reaction model Part 1: batch solution process, J. Appl. Polym. Sci. 102 (2) (2006) 1182–1190.
[22] J.M. García-Martínez, S. Areso, E. Collar, The transient nature of maximum maleic anhydride grafting of polypropylene: a mechanistic approach based on a consecutive reaction model. II. A comparison of the batch solution and molten state processes, J. Appl. Polym. Sci. 104 (1) (2007) 345–351.
[23] A. Bhattacharya, S. Mondal, A. Bandyopadhyay, Maleic anhydride grafted atactic polypropylene as exciting new compatibilizer for poly (ethylene-co-octene) organically modified clay nanocomposites: investigations on mechanical and rheological properties, Ind. Eng. Chem. Res. 52 (39) (2013) 14143–14153.
[24] J. Qian, Z. Huang, S. Dang, Y. Xu, Improvements of polypropylene grafted maleic anhydride with ultrasonication, pre-irradiation and co-irradiation methods, J. Polym. Res. 18 (6) (2011) 1557–1565.
[25] F. Kučera, J. Petruš, P. Poláček, J. Jančář, Controlled reactive modification of polypropylene with maleic anhydride via solvent-free technique, Polym. Degrad. Stabil. 168 (2019), 108934.
[26] M.F. Diop, J.M. Torkelson, Maleic anhydride functionalization of polypropylene with suppressed molecular weight reduction via solid-state shear pulverization, Polymer 54 (16) (2013) 4143–4154.
[27] L. Krause-Sammartino, J. Lucas, M. Reboredo, M. Aranguren, Maleic anhydride grafting of polypropylene: peroxide and solvent effects, Plast., Rubber Compos. 35 (3) (2006) 117–123.
[28] J. Roeder, R. Oliveira, M. Gonçalves, V. Soldi, A. Pires, Polypropylene/polyamide-6 blends: influence of compatibilizing agent on interface domains, Polym. Test. 21 (7) (2002) 815–821.
[29] J.D. Tucker, S. Lee, R.L. Einsporn, A study of the effect of PP-g-MA and SEBS-g-MA on the mechanical and morphological properties of polypropylene/nylon 6 blends, Polym. Eng. Sci. 40 (12) (2000) 2577–2589.
[30] S.N. Sathe, S. Devi, G.S. Rao, K. Rao, Relationship between morphology and mechanical properties of binary and compatibilized ternary blends of polypropylene and nylon 6, J. Appl. Polym. Sci. 61 (1) (1996) 97–107.
[31] J.M. García-Martínez, E.P. Collar, Industrial waste origin succinic anhydride-grafted atactic polypropylene as compatibilizer of full range polypropylene/polyamide 6 blends as revealed by dynamic mechanical analysis at the polypropylene glass transition, Polym. Eng. Sci. 59 (12) (2019) 2458–2466.
[32] E. Collar, J. Taranco, S. Areso, J.M. García-Martínez, Understanding the morphological changes in the polypropylene/polyamide 6 fifty/fifty blends by interfacial modifiers based on grafted atactic polypropylenes: microscopic, mechanical, and thermal characterization, J. Polym. 2015 (2015).
[33] Y.H. Hu, C.Y. Chen, C.C. Wang, Y.H. Huang, S.P. Wang, Living polymerization of styrene initiated by mercaptan/ε-caprolactam, J. Polym. Sci. Polym. Chem. 42 (19) (2004) 4976–4993.
[34] C.-Y. Hung, C.-C. Wang, C.-Y. Chen, Enhanced the thermal stability and crystallinity of polylactic acid (PLA) by incorporated reactive PS-b-PMMA-b-PGMA and PS-b-PGMA block copolymers as chain extenders, Polymer 54 (7) (2013) 1860–1866.
[35] C.P. Wu, C.C. Wang, C.Y. Chen, Enhancing the PLA crystallization rate by incorporating a polystyrene-block-poly (methyl methacrylate) block copolymer: synergy of polystyrene and poly (methyl methacrylate) segments, J. Polym. Sci. B Polym. Phys. 52 (12) (2014) 823–832.

[36] C.-P. Wu, C.-C. Wang, C.-Y. Chen, Influence of asymmetric ratio of polystyrene-block-poly (methyl methacrylate) block copolymer on the crystallization rate of PLA, Eur. Polym. J. 66 (2015) 160–169.
[37] C.-P. Wu, C.-C. Wang, C.-Y. Chen, Investigation of mercaptan/ε-caprolactam initiated bulk copolymerization of methyl methacrylate with vinyl monomers, J. Polym. Res. 26 (4) (2019) 94.
[38] B. De Roover, M. Sclavons, V. Carlier, J. Devaux, R. Legras, A. Momtaz, Molecular characterization of maleic anhydride-functionalized polypropylene, J. Polym. Sci. Polym. Chem. 33 (5) (1995) 829–842.
[39] M. Morra, E. Occhiello, F. Garbassi, Contact angle hysteresis on oxygen plasma treated polypropylene surfaces, J. Colloid Interface Sci. 132 (2) (1989) 504–508.
[40] S.N. Sathe, G.S. Rao, S. Devi, Grafting of maleic anhydride onto polypropylene: synthesis and characterization, J. Appl. Polym. Sci. 53 (2) (1994) 239–245.
[41] Y. Seo, J. Kim, K.U. Kim, Y.C. Kim, Study of the crystallization behaviors of polypropylene and maleic anhydride grafted polypropylene, Polymer 41 (7) (2000) 2639–2646.
[42] A.R. Bhattacharyya, T. Sreekumar, T. Liu, S. Kumar, L.M. Ericson, R.H. Hauge, R. E. Smalley, Crystallization and orientation studies in polypropylene/single wall carbon nanotube composite, Polymer 44 (8) (2003) 2373–2377.
[43] J.-H. Chen, F.-C. Tsai, Y.-H. Nien, P.-H. Yeh, Isothermal crystallization of isotactic polypropylene blended with low molecular weight atactic polypropylene. Part I. Thermal properties and morphology development, Polymer 46 (15) (2005) 5680–5688.